

## Interference in the $gg \rightarrow h \rightarrow \gamma\gamma$ On-Shell Rate and the Higgs Boson Total Width

John Campbell,<sup>1</sup> Marcela Carena,<sup>1,2,3</sup> Roni Harnik,<sup>1</sup> and Zhen Liu<sup>1</sup>

<sup>1</sup>Theoretical Physics Department, Fermilab, Batavia, Illinois 60510, USA

<sup>2</sup>Enrico Fermi Institute, University of Chicago, Chicago, Illinois 60637, USA

<sup>3</sup>Kavli Institute for Cosmological Physics, University of Chicago, Chicago, Illinois 60637, USA

(Received 26 May 2017; published 30 October 2017; publisher error corrected 31 October 2017)

We consider interference between the Higgs signal and QCD background in  $gg \rightarrow h \rightarrow \gamma\gamma$  and its effect on the on-shell Higgs rate. The existence of sizable strong phases leads to destructive interference of about 2% of the on-shell cross section in the standard model. This effect can be enhanced by beyond the standard model physics. In particular, since it scales differently from the usual rates, the presence of interference allows indirect limits to be placed on the Higgs width in a novel way, using on-shell rate measurements. Our study motivates further QCD calculations to reduce uncertainties. We discuss possible width-sensitive observables, both using total and differential rates and find that the HL-LHC can potentially indirectly constrain widths of order tens of MeV.

DOI: 10.1103/PhysRevLett.119.181801

*Introduction.*—The recent discovery of a standard model (SM)-like Higgs boson at the LHC opens a new era of research in particle physics. The Higgs boson is directly connected to the origin of mass of fundamental particles and the electroweak scale. Therefore, precision tests of the properties of the Higgs boson provide a unique window into these basic questions. At the LHC, the current sensitivity in the cleanest Higgs boson channels is already exceeding expectations, while projections for future sensitivity after the high luminosity LHC (HL-LHC) run are at the few percent level [1,2]. In anticipation of the coming era of high precision Higgs physics, small effects in Higgs production and decay rates should be carefully scrutinized, and together with new observables, they may shed light on beyond the standard model effects encoded in the Higgs partial and total decay widths.

In this Letter, we explore the physics potential for constraining the SM Higgs total decay width from the change in on-shell Higgs rates due to interference effects between the Higgs signal and the QCD background. This change in rates requires the existence of a so-called strong phase in the amplitudes, that can be present both in the Higgs signal and in the continuum background, as is the case in the SM. We shall demonstrate that, the different scaling behavior between the strong phase induced interference and the Breit-Wigner parts of the on-shell Higgs rate may allow the placement of bounds on, or even measurements of, the Higgs boson total width. Both theoretical and experimental uncertainties are the leading limiting factors in this program. On the other hand, without the strong phase induced interference effects, fits to on-shell Higgs rates can only place bounds on the total width by making definite theoretical assumptions [3–5].

In the following we shall focus on the process  $gg \rightarrow h \rightarrow \gamma\gamma$ , which will be measured with very high precision at the LHC. The interference effect affecting the

Higgs production rate through this process was estimated more than a decade ago in Refs. [6,7]. We explore this effect further and highlight for the first time the resulting sensitivity to the Higgs boson total decay width. We study the change in the cross section as a function of a veto on the Higgs boson transverse momentum and as a function of the photon scattering angle in the diphoton rest frame. More recently, interference effects in this channel have been studied extensively in Refs. [8–11], putting the main emphasis on the interference part proportional to the real component of the scalar propagator that shifts the Higgs diphoton invariant mass peak at the +10 to –70 MeV level, depending on the cuts. The interference effect investigated in this work is complementary to those studies in the sense that it is proportional to the imaginary component of the propagator and provides information on the Higgs total decay width from an on-shell Higgs boson cross section measurement. Our effect is also complementary to the off-shell method [12–14], since it is independent of new physics effects that may distort the measurements in the far off-shell region.

*Interference effects and sensitivity to the Higgs width.*—To quantify the effect of the Higgs boson on the diphoton production rate, including the effect of interference with QCD background, we compute observables based on the following combination of amplitudes,

$$\begin{aligned} |\mathcal{M}_h|^2 &= |A_h + A_{\text{bkg}}|^2 - |A_{\text{bkg}}|^2 \\ &= |A_h|^2 + 2\text{Re}[A_h A_{\text{bkg}}^*], \end{aligned} \quad (1)$$

where  $A_h$  and  $A_{\text{bkg}}$  are amplitudes for diphoton production through an  $s$ -channel Higgs signal and for the rest of the interfering SM processes, respectively. For simplicity, helicity indices are suppressed in this section. In the following it is useful to write the amplitude for  $gg \rightarrow h \rightarrow \gamma\gamma$  in a form which explicitly factors out the loop-induced

couplings to gluons ( $F_{gg}$ ) and photons ( $F_{\gamma\gamma}$ ), (The use of alternatives to the Breit-Wigner form used here, such as the scheme advocated in Ref. [15], would lead to differences much smaller than one per mille to the on-shell rate.)

$$A_h \equiv A_{gg \rightarrow h \rightarrow \gamma\gamma} \propto \frac{\hat{s}}{\hat{s} - m_h^2 + i\Gamma_h m_h} F_{gg} F_{\gamma\gamma}. \quad (2)$$

Considering Eq. (1), the interference term can come from different contributions. Taking both  $F_{gg}$  and  $F_{\gamma\gamma}$  as real Wilson coefficients of effective vertices is sufficient for most purposes. In such a case,  $A_h$  is purely imaginary when exactly on shell,  $\hat{s} = m_h^2$ . In addition, the phase of the leading order QCD background amplitude for  $gg \rightarrow \gamma\gamma$  is often neglected. These two approximations imply that the interference term in Eq. (1) vanishes at  $\hat{s} = m_h^2$ . Moreover, under the above conditions, the interference term is proportional to the real part of  $A_h$ , and hence an odd function of  $\hat{s} - m_h^2$ . Therefore, upon  $d\hat{s}$  integration the interference term does not change the overall rate but rather shifts in the location of the peak [8–11]. (This argument is correct up to very small corrections due to the slope of the PDF and a slight  $\hat{s}$  dependence for the interference term that generates an asymmetric contribution around the pole. These effects are parametrically much smaller than the effect we will study, thus are neglected here.)

Interestingly, a careful inspection of additional contributions to the interference term reveals effects that are not captured in the above discussion. Both the Higgs couplings  $F_{gg}$  and  $F_{\gamma\gamma}$  as well as the background amplitude  $A_{\text{bkg}}$  receive absorptive contributions that arise from loops of particles that are sufficiently light to be on shell. The resulting induced phases are usually dubbed “strong phases” in the flavor literature and we will adopt this terminology here. (Strong phases, which are  $CP$  even get their name because they often arise in flavor physics from QCD dynamics. This is in contrast with  $CP$  odd weak phases, e.g., the relative size of the Higgs couplings to  $F\tilde{F}$  versus  $FF$ .) In the presence of a strong phase we can write the interference term as

$$|\mathcal{M}_h|_{\text{int}}^2 \equiv 2\text{Re}[A_h A_{\text{bkg}}^*] = \frac{2|A_{\text{bkg}}||F_{gg}||F_{\gamma\gamma}|}{(\hat{s} - m_h^2)^2 + \Gamma_h^2 m_h^2} \times [(\hat{s} - m_h^2) \cos(\delta_{\text{bkg}} - \delta_h) + m_h \Gamma_h \sin(\delta_{\text{bkg}} - \delta_h)], \quad (3)$$

where we have taken  $\delta_h = \arg[F_{gg}] + \arg[F_{\gamma\gamma}]$  and  $\delta_{\text{bkg}} = \arg[A_{\text{bkg}}]$  as the signal and background strong phases, respectively. The first term in the square bracket is the contribution to the interference term that, as we discussed below Eq. (2), does not modify the overall rate upon integration over  $\hat{s}$ . The second term is the subject of this work and leads to a modified rate in the presence of a strong

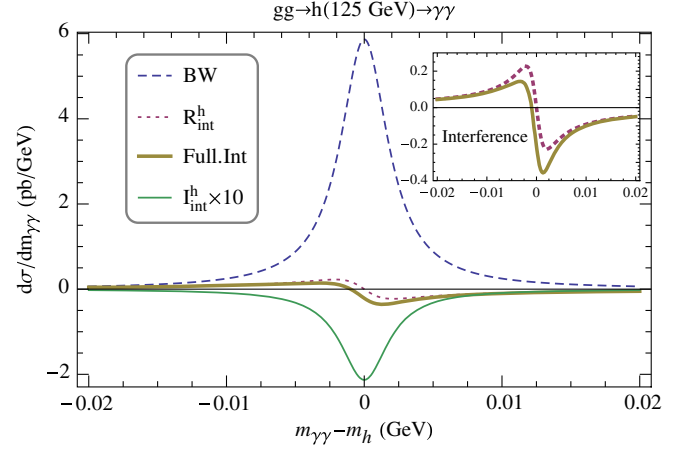


FIG. 1. The line shape induced by various contributions to the cross section for  $gg \rightarrow h \rightarrow \gamma\gamma$  in the SM. The Breit-Wigner line shape, with no interference, is shown in blue (dashed line), while the effects of  $\mathcal{R}_h^{\text{int}}$  and  $\mathcal{I}_h^{\text{int}}$  (multiplied by a factor of 10) are shown in red (dotted line) and green (solid line), respectively. The overall effect of the interference in the full NLO calculation is given by the brown (solid) line. The inset in the top right is a magnification of the corresponding interference line shapes.

phase. For convenience, we define  $|\mathcal{M}_h|_{\text{int}}^2 = \mathcal{R}_h^{\text{int}} + \mathcal{I}_h^{\text{int}}$  and  $\delta_s = \delta_{\text{bkg}} - \delta_h$  such that

$$\begin{aligned} \mathcal{R}_h^{\text{int}} &\equiv \frac{2|A_{\text{bkg}}||F_{gg}||F_{\gamma\gamma}|}{(\hat{s} - m_h^2)^2 + \Gamma_h^2 m_h^2} (\hat{s} - m_h^2) \cos \delta_s, \\ \mathcal{I}_h^{\text{int}} &\equiv \frac{2|A_{\text{bkg}}||F_{gg}||F_{\gamma\gamma}|}{(\hat{s} - m_h^2)^2 + \Gamma_h^2 m_h^2} m_h \Gamma_h \sin \delta_s. \end{aligned} \quad (4)$$

In the SM the dominant contribution to  $\mathcal{I}_h^{\text{int}}$  comes from the phase of the background amplitude at two loops [6,7]. The signal amplitude also contains a strong phase, mainly due to bottom quark loops. We have performed a calculation of the interference effect that accounts for absorptive effects from both signal and background. In Fig. 1 we illustrate the features of the interference effects. The line shape, the differential cross section as a function of  $\hat{s}$ , is shown for the pure Breit-Wigner (only  $|A_h|^2$ ), and for the interference contributions  $\mathcal{I}_h^{\text{int}}$  and  $\mathcal{R}_h^{\text{int}}$  as well as for the sum of both. For visualization, the interference contribution  $\mathcal{I}_h^{\text{int}}$  has been magnified by a factor of 10. In this figure we show the line shapes obtained including NLO effects with virtual corrections only. After summing over different interfering helicity amplitudes, we obtain averaged strong phases  $\delta_h = (\pi + 0.036)$  and  $\delta_{\text{bkg}} = -0.205$  for the signal and background, respectively.

Given that the interference term  $\mathcal{I}_h^{\text{int}}$  and the Breit-Wigner term have a different dependence on the Higgs boson total width and most other on-shell Higgs cross sections are with negligible interference contribution, it follows that the on-shell cross section of  $gg \rightarrow h \rightarrow \gamma\gamma$  gains sensitivity to the total width. Schematically,

$$\begin{aligned} \sigma &\sim \int dm_{\gamma\gamma} \frac{|F_{gg}|^2 |F_{\gamma\gamma}|^2}{(\hat{s} - m_h^2)^2 + \Gamma_h^2 m_h^2} \\ &\times \left( 1 + \frac{2|A_{\text{bkg}}| [(\hat{s} - m_h^2) \cos \delta_s + m_h \Gamma_h \sin \delta_s]}{|F_{gg}| |F_{\gamma\gamma}|} \right) \\ &\propto \frac{|F_{gg}|^2 |F_{\gamma\gamma}|^2}{\Gamma_h m_h} \left( 1 + \frac{2m_h \Gamma_h |A_{\text{bkg}}| \sin \delta_s}{|F_{gg}| |F_{\gamma\gamma}|} \right). \end{aligned} \quad (5)$$

This equation can be identified as expressing the parametric dependence of the cross section in the form of  $\sigma = \sigma_{\text{BW}}(1 + \sigma_{\text{int}}/\sigma_{\text{BW}})$ . The first term in this equation displays the usual dependence of an on-shell cross section on the decay width, identical to that of the narrow-width-approximation result. In the absence of the interference effect it implies that such cross sections are insensitive to simultaneous changes to the Higgs couplings and total width that leave the quantity  $|F_{gg}|^2 |F_{\gamma\gamma}|^2 / \Gamma_h$  invariant—this is the so-called flat direction in this parameter space. Combining the  $\gamma\gamma$  rate with other channels will not eliminate this ambiguity since all on-shell rates exhibit an identical scaling with the corresponding couplings, namely,  $g_i^2 g_f^2 / \Gamma_h$ , where  $g_i$  and  $g_f$  are the couplings for production and decay of the corresponding channel, respectively. However the presence of the second interference term in Eq. (5) lifts this degeneracy. This special dependence on the total width can, in the fullness of time, be exploited by global fits of experimental data that determine Higgs properties.

As a concrete example that demonstrates the potential of this novel effect, without loss of generality we can consider excursions in the flat direction corresponding to

$$\frac{|F_{gg}|^2 |F_{\gamma\gamma}|^2}{|F_{gg}^{\text{SM}}|^2 |F_{\gamma\gamma}^{\text{SM}}|^2} = \frac{\Gamma_h}{\Gamma_h^{\text{SM}}}. \quad (6)$$

The total Higgs cross section can then be written as

$$\sigma = \sigma_{\text{BW}}^{\text{SM}} \left( 1 + \frac{\sigma_{\text{int}}^{\text{SM}}}{\sigma_{\text{BW}}^{\text{SM}}} \sqrt{\frac{\Gamma_h}{\Gamma_h^{\text{SM}}}} \right) \approx \sigma_{\text{BW}}^{\text{SM}} \left( 1 - 2\% \sqrt{\frac{\Gamma_h}{\Gamma_h^{\text{SM}}}} \right). \quad (7)$$

The results of a full NLO calculation of the interference effect are presented in Fig. 2, which shows the relative size of the interference effect as a function of the total width, normalized to its SM value, for parameter excursions defined by Eq. (6). (For details of the NLO calculation, see the Supplemental Material [16] with Refs [17–29].) The variation of the interference effect with the total width is shown imposing a 20 GeV  $p_T^h$  veto, with and without LHC cuts on the final state photons. Since the interference effect is largest at small scattering angles (see Fig. 3), the photon cuts reduce the expected interference. This small consideration in the SM leads to much bigger differences for  $\Gamma_h \gg \Gamma_h^{\text{SM}}$ . Observe that in the SM the interference contribution is destructive. However, if the sign of  $F_{gg} F_{\gamma\gamma}$  were flipped, ( $\delta_s \rightarrow \pi + \delta_s$ ), the interference effect would lead to an enhancement of the diphoton rate rather than a

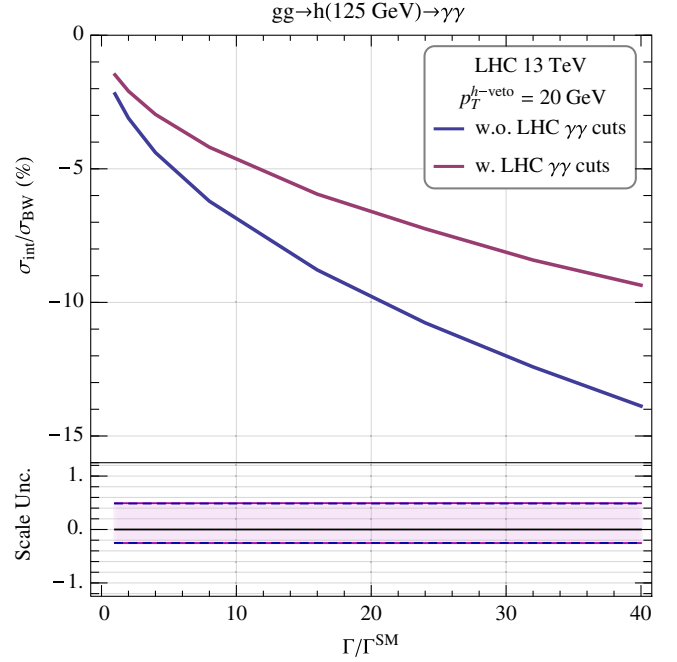


FIG. 2. The total signal rate change due to the interference effect as a function of the Higgs total width normalized to its SM value, while keeping the Breit-Wigner cross section identical to that of the SM Higgs. The magenta and blue (solid) lines represent the cases with and without LHC cuts on the final state photons, respectively. The lower panel shows the scale variation uncertainties for these interference terms as bands delimited by the blue (dashed) and magenta (solid) lines. The curves are obtained with a veto on the Higgs boson  $p_T$  at 20 GeV.

suppression. The theoretical scale uncertainty is shown in the bottom panel of Fig. 2 and amounts to about  $^{+50\%}_{-30\%}$ . For example, the interference effect is  $-(2.20^{+1.06}_{-0.55})\%$  without photon cuts for the SM Higgs boson. Although a measurement at the 2% level may be challenging at the LHC, this shows that a precise measurement of the  $gg \rightarrow h \rightarrow \gamma\gamma$  rate can place a limit on the width of the Higgs boson. In this respect, a measurement of the ratio of the  $\gamma\gamma$  rate to the  $4\ell$  rate is a promising route to reduce many of the systematic and theoretical, e.g., PDF and other parametric, uncertainties.

*Kinematic dependence of the interference.*—It is important to understand the variation of the interference effect with kinematic variables. In Fig. 3 we show the differential distribution of the ratio  $\sigma_{\text{int}}/\sigma_{\text{BW}}$  as a function of the photon scattering angle (in the  $\gamma\gamma$  rest frame) for different orders of the signal and background amplitudes for the SM Higgs boson. The brown dotted line shows the interference effect at LO (1-loop) in both signal and background, but without including the signal strong phase. Staying at this order, but now including the strong phase in the Higgs amplitude leads to a somewhat larger effect, shown by the green dashed line. The background strong phase is suppressed by the masses of light quarks at one loop, but this suppression is absent at the two loop level. We therefore see a sizable

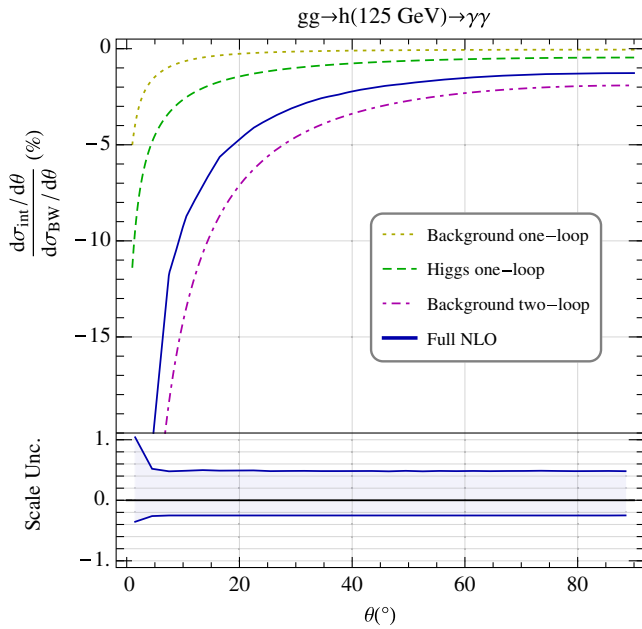


FIG. 3. Parton level cross section change due to the interference effect as a function of the photon scattering angle in the diphoton rest frame for the SM Higgs. The full NLO result is shown in the solid blue curve. The blue band in the lower panel represents the scale uncertainty in the calculation of this effect. The dotted, dashed, and dot-dashed lines correspond to partial calculations where the strong phase is included at various orders (see text). The partial calculations include only virtual corrections while the full calculation result includes a Higgs  $p_T$  veto of 20 GeV.

enhancement in this interference effect once we include the background amplitude at two loops (magenta, dot-dashed line). This curve is similar to the estimate of Ref. [7]. The full NLO calculation is shown by the solid blue line. The slight dilution of the effect going from the dot-dashed line to full NLO originates from an enhancement of  $\sigma_{\text{BW}}$  from real emission effects. For all curves we see that the interference effect is largest in the forward direction due to the kinematic behavior of the interfering background in this region.

*Strategies for constraining the Higgs boson width.*—The most straightforward approach is to compare the on-shell Higgs rate to the standard model prediction, with and without the inclusion of the interference term. The different parametric dependence of the Breit-Wigner and interference terms would allow us to access the Higgs total width. The HL-LHC projections for the statistical uncertainty in the rate of the 0-jet and 1-jet tagged Higgs boson to diphoton channels are 4% and 5%, respectively [2]. These measurements, however, are dominated by larger systematic and theoretical uncertainties, including those of beam luminosity and PDF. The best measured channels at the LHC,  $gg \rightarrow h \rightarrow \gamma\gamma$  and  $gg \rightarrow h \rightarrow 4\ell$ , provide the most accurate cross section ratio, projected to be measurable at the 4% level [2]. In contrast to single cross section measurements, the precision on this ratio is statistically limited. We observe, however, that if we naively scale the

statistical uncertainty from the 8 TeV measurement [30] as the square root of the number of events, one reaches an impressive statistical uncertainty of 1%–1.5% at the HL-LHC. Together with the potential for improved analyses, it is not unreasonable to have high expectations for future HL-LHC performance. Regardless of the ultimate reach of the HL-LHC, a few percent level is interestingly within striking distance of this novel interference effect.

Keeping the current theoretical uncertainty band in mind, the projected sensitivity of 4% on the ratio of  $\gamma\gamma$  to  $4\ell$  yields can be translated into an upper limit of 22, 14, and 8 on  $\Gamma_h/\Gamma_h^{\text{SM}}$  at the  $1\sigma$  level, for low, central, and high theoretical expectations on this interference effect, respectively. (This limit is worse by 1 order of magnitude than the off-shell Higgs measurement that constrains the Higgs total width [12–14]. However, unlike the off-shell Higgs measurement, our effect is independent from the assumptions on the high-energy behavior of the Higgs boson and the absence of new physics contribution in the off-shell region. For more detailed discussion, see, e.g., Chap. I.8 of the Higgs Yellow Report [31] and Refs. [32,33].) These expected sensitivities assume the observed measurement will agree with the standard model prediction, including our interference effect. This also assumes that the couplings to photons and Z bosons maintain their SM ratio and the photon and gluon couplings respect Eq. (6). The Higgs cross section precisions are anticipated to improve by at least 1 order of magnitude at a future circular  $pp$  collider [34,35]. This can be naively translated into lower and upper limits on the Higgs total width of  $0.5 < \Gamma_h/\Gamma_h^{\text{SM}} < 1.6$  at  $1\sigma$  level using the central value from our NLO theory calculation. This high level of precision may thus establish the existence of the interference effect at the  $3\sigma$  level and differential distribution study will further improve it. (Although the Higgs total width might be measured well by future lepton colliders, our interference effect would still be important for precision studies of the  $gg \rightarrow H \rightarrow \gamma\gamma$  process at the FCC-hh. For example, our interference effect, together with the diphoton invariant mass shift [8–11], would test the Higgs amplitude in both its  $\mathcal{T}_h^{\text{int}}$  and  $\mathcal{R}_h^{\text{int}}$  components. Furthermore, our effect will be sensitive to  $CP$ -violation effects in the gluon-gluon-Higgs coupling at the Higgs mass, which can hardly be tested elsewhere. We leave this for future work.)

The interference effect on the total rate cannot be measured separately from the rate itself. Therefore, it is important to consider strategies for limiting the size of the interference effect independent of a flat direction or any additional theory input for the ratio of the Higgs boson branching fractions. The effects of interference can be measured independently from the rate by probing its dependence on kinematic observables such as the scattering angle shown in Figs. 3. The best sensitivity to this effect would presumably be achieved by employing a multivariate analysis on the data. Here we will simply consider a coarse binning of these distributions that can be compared with data as the precision improves.

TABLE I. The effect of the interference in bins of the photon polar angle in the Higgs rest frame. The effect is shown for three cases: no cuts, only a  $p_T^h$  veto of 20 GeV, and LHC photon cuts in addition to the  $p_T^h$  veto. The scale uncertainties are correlated across the various bins. Furthermore, the size of the effect grows uniformly in all table entries as  $\sim\sqrt{\Gamma/\Gamma_{\text{SM}}}$ , for parameter excursions in which all other Higgs yields are held fixed.

$ \cos\theta $	$-\sigma_{\text{int}}/\sigma_{\text{BW}}$ (%)		
	no cuts	$p_T^h$ veto	$\gamma\gamma$ cuts + veto
0.0–0.2	$0.87^{+0.34}_{-0.20}$	$1.28^{+0.62}_{-0.32}$	$1.34^{+0.68}_{-0.34}$
0.2–0.4	$0.91^{+0.36}_{-0.21}$	$1.35^{+0.65}_{-0.34}$	$1.41^{+0.72}_{-0.36}$
0.4–0.6	$1.04^{+0.41}_{-0.24}$	$1.53^{+0.74}_{-0.38}$	$1.62^{+0.83}_{-0.42}$
0.6–0.8	$1.37^{+0.53}_{-0.31}$	$1.99^{+0.96}_{-0.50}$	$1.65^{+0.75}_{-0.40}$
0.8–1.0	$3.55^{+1.45}_{-0.82}$	$4.85^{+2.37}_{-1.23}$	...
0.0–1.0	$1.52^{+0.60}_{-0.35}$	$2.20^{+1.06}_{-0.55}$	$1.48^{+0.73}_{-0.38}$

The isotropic nature of the Higgs boson decay means that, in principle, the interference effect can be mapped out by measuring the photon polar angle in the Higgs boson rest frame. Table I shows the size of the interference effect, as a fraction of the Breit-Wigner part of the Higgs boson signal, for a few bins in  $|\cos\theta|$ . Here we consider three selection criteria—the application of no cuts at all, no photon cuts but the application of our Higgs  $p_T$  veto, and, finally, our LHC photon cuts together with the veto. We will not attempt to estimate the reach of this analysis method. However, observe that, for the  $2 \rightarrow 2$  scattering configurations that dominate the interference effect, the value of  $|\cos\theta|$  is constrained by the photon selection cuts. It would be possible to observe a significantly larger interference if the photon acceptance coverage were enlarged.

*Conclusion.*—In this Letter we discuss the change in the  $gg \rightarrow h \rightarrow \gamma\gamma$  on-shell rate, due to interference between the Higgs signal and the QCD background amplitudes, as a way to provide a novel handle to constrain—or even measure—the Higgs boson total width. We perform a full NLO calculation at order  $\alpha_s^3$  of the interference effect and find that in the standard model it leads to a reduction of the on-shell rate by  $\sim 2\%$ . The proposed method for gaining sensitivity to the Higgs boson width is complementary to other methods that have been discussed in the literature. Altogether, our study aims at motivating a more thorough examination of Higgs precision physics taking into account the strong phase induced interference effect in different Higgs boson observables.

This manuscript has been co-authored by employees of the Fermi Research Alliance, LLC under Contract No. DE-AC02-07CH11359 with the U.S. Department of Energy, Office of Science, Office of High Energy Physics. The U.S. Government retains and the publisher, by accepting the article for publication, acknowledges that the U.S.

Government retains a non-exclusive, paid-up, irrevocable, world-wide license to publish or reproduce the published form of this manuscript, or allow others to do so, for U.S. Government purposes.

- [1] S. Dawson *et al.*, Working Group Report: Higgs Boson, Proceedings of the 2013 Community Summer Study on the Future of U.S. Particle Physics: Snowmass on the Mississippi (CSS2013): Minneapolis, MN, USA, 2013, <http://inspirehep.net/record/1262795/files/arXiv:1310.8361.pdf>.
- [2] The ATLAS Collaboration, Technical Report ATL-PHYS-PUB-2014-016, CERN, Geneva, 2014, <http://cds.cern.ch/record/1956710>.
- [3] M. Dührssen, S. Heinemeyer, H. Logan, D. Rainwater, G. Weiglein, and D. Zeppenfeld, Extracting Higgs boson couplings from CERN LHC data, *Phys. Rev. D* **70**, 113009 (2004).
- [4] A. David, A. Denner, M. Dührssen, M. Grazzini, C. Grojean, G. Passarino, M. Schumacher, M. Spira, G. Weiglein, and M. Zanetti (LHC Higgs Cross Section Working Group Collaboration), LHC HXSWG interim recommendations to explore the coupling structure of a Higgs-like particle, [arXiv:1209.0040](https://arxiv.org/abs/1209.0040).
- [5] B. A. Dobrescu and J. D. Lykken, Coupling spans of the Higgs-like boson, *J. High Energy Phys.* **02** (2013) 073.
- [6] D. A. Dicus and S. S. D. Willenbrock, Photon pair production and the intermediate mass Higgs boson, *Phys. Rev. D* **37**, 1801 (1988).
- [7] L. J. Dixon and M. S. Siu, Resonance Continuum Interference in the Diphoton Higgs Signal at the LHC, *Phys. Rev. Lett.* **90**, 252001 (2003).
- [8] S. P. Martin, Shift in the LHC Higgs diphoton mass peak from interference with background, *Phys. Rev. D* **86**, 073016 (2012).
- [9] S. P. Martin, Interference of Higgs diphoton signal and background in production with a jet at the LHC, *Phys. Rev. D* **88**, 013004 (2013).
- [10] L. J. Dixon and Y. Li, Bounding the Higgs Boson Width Through Interferometry, *Phys. Rev. Lett.* **111**, 111802 (2013).
- [11] F. Coradeschi, D. de Florian, L. J. Dixon, N. Fianza, S. Höche, H. Ita, Y. Li, and J. Mazzitelli, Interference effects in the  $H(\rightarrow\gamma\gamma) + 2$  jets channel at the LHC, *Phys. Rev. D* **92**, 013004 (2015).
- [12] N. Kauer and G. Passarino, Inadequacy of zero-width approximation for a light Higgs boson signal, *J. High Energy Phys.* **08** (2012) 116.
- [13] F. Caola and K. Melnikov, Constraining the Higgs boson width with ZZ production at the LHC, *Phys. Rev. D* **88**, 054024 (2013).
- [14] J. M. Campbell, R. K. Ellis, and C. Williams, Bounding the Higgs width at the LHC using full analytic results for  $gg \rightarrow e^-e^+\mu^-\mu^+$ , *J. High Energy Phys.* **04** (2014) 060.
- [15] G. Passarino, C. Sturm, and S. Uccirati, Higgs pseudo-observables, second Riemann sheet and all that, *Nucl. Phys.* **B834**, 77 (2010).
- [16] See Supplemental Material at <http://link.aps.org/supplemental/10.1103/PhysRevLett.119.181801> for details

- for the amplitudes decomposition, NLO calculation, input parameters, and additional kinematic features.
- [17] Z. Bern and D.A. Kosower, The computation of loop amplitudes in gauge theories, *Nucl. Phys.* **B379**, 451 (1992).
- [18] Z. Bern, A. De Freitas, and L.J. Dixon, Two loop amplitudes for gluon fusion into two photons, *J. High Energy Phys.* **09** (2001) 037.
- [19] Z. Bern and A. G. Morgan, Massive loop amplitudes from unitarity, *Nucl. Phys.* **B467**, 479 (1996).
- [20] Z. Bern, L.J. Dixon, and D.A. Kosower, One Loop Corrections to Five Gluon Amplitudes, *Phys. Rev. Lett.* **70**, 2677 (1993).
- [21] Z. Bern, L.J. Dixon, and C. Schmidt, Isolating a light Higgs boson from the diphoton background at the CERN LHC, *Phys. Rev. D* **66**, 074018 (2002).
- [22] D. de Florian, N. Fianza, R.J. Hernandez-Pinto, J. Mazzitelli, Y. Rotstein Habarnau, and G.F.R. Sborlini, A complete  $O(\alpha_s^2)$  calculation of the signal-background interference for the Higgs diphoton decay channel, *Eur. Phys. J. C* **73**, 2387 (2013).
- [23] S. Catani and M.H. Seymour, A general algorithm for calculating jet cross sections in NLO QCD, *Nucl. Phys.* **B485**, 291 (1997); Erratum, *Nucl. Phys.* **B510**, 503 (1998).
- [24] J.M. Campbell, R.K. Ellis, and C. Williams, Vector boson pair production at the LHC, *J. High Energy Phys.* **07** (2011) 018.
- [25] S. Dulat, T.-J. Hou, J. Gao, M. Guzzi, J. Huston, P. Nadolsky, J. Pumplin, C. Schmidt, D. Stump, and C.P. Yuan, New parton distribution functions from a global analysis of quantum chromodynamics, *Phys. Rev. D* **93**, 033006 (2016).
- [26] A. Djouadi, P. Gambino, and B.A. Kniehl, Two loop electroweak heavy fermion corrections to Higgs boson production and decay, *Nucl. Phys.* **B523**, 17 (1998).
- [27] G. Degrandi and F. Maltoni, Two-loop electroweak corrections to the Higgs-boson decay  $H \rightarrow \gamma\gamma$ , *Nucl. Phys.* **B724**, 183 (2005).
- [28] G. Passarino, C. Sturm, and S. Uccirati, Complete two-loop corrections to  $H \rightarrow \gamma\gamma$ , *Phys. Lett. B* **655**, 298 (2007).
- [29] S. Dittmaier *et al.* (LHC Higgs Cross Section Working Group Collaboration), Handbook of LHC Higgs cross sections: 1. Inclusive observables, [arXiv:1101.0593](https://arxiv.org/abs/1101.0593).
- [30] G. Aad *et al.* (ATLAS, CMS Collaborations), Measurements of the Higgs boson production and decay rates and constraints on its couplings from a combined ATLAS and CMS analysis of the LHC pp collision data at  $\sqrt{s} = 7$  and 8 TeV, *J. High Energy Phys.* **08** (2016) 045.
- [31] D. de Florian *et al.* (LHC Higgs Cross Section Working Group Collaboration), Handbook of LHC Higgs Cross Sections: 4. Deciphering the Nature of the Higgs Sector, [arXiv:1610.07922](https://arxiv.org/abs/1610.07922).
- [32] C. Englert and M. Spannowsky, Limitations and opportunities of off-shell coupling measurements, *Phys. Rev. D* **90**, 053003 (2014).
- [33] H.E. Logan, Hiding a Higgs width enhancement from off-shell  $gg(\rightarrow h^*) \rightarrow ZZ$  measurements, *Phys. Rev. D* **92**, 075038 (2015).
- [34] N. Arkani-Hamed, T. Han, M. Mangano, and L.-T. Wang, Physics opportunities of a 100 TeV proton-proton collider, *Phys. Rep.* **652**, 1 (2016).
- [35] R. Contino *et al.*, Physics at a 100 TeV pp collider: Higgs and EW symmetry breaking studies, [arXiv:1606.09408](https://arxiv.org/abs/1606.09408).